Environmental Science Nano

PAPER

View Article Online
View Journal | View Issue

Cite this: *Environ. Sci.: Nano*, 2016, 3, 1280

Visualization tool for correlating nanomaterial properties and biological responses in zebrafish†

Sandra C. Karcher,*[ae] Bryan J. Harper,[b] Stacey L. Harper,[b] Christine Ogilvie Hendren,[ce] Mark R. Wiesner[ce] and Gregory V. Lowry*[de]

Received 21st July 2016,
Accepted 15th September 2016

DOI: 10.1039/c6en00273k

rsc.li/es-nano

The complexity of engineered nanomaterials with regard to their structure and system-dependent properties, and limits of instrumentation to fully characterize nanomaterials in aqueous suspensions or biological media make it difficult to understand how material structure invokes biological response. In this work, a data visualization tool was developed to explore the results of 151 zebrafish assays stored in the Nanomaterial-Biological Interactions Knowledgebase. Visualizations generated using the tool indicated that some nanomaterials exhibited a tendency to cause death, others, sublethal abnormalities. The visualizations also showed that combinations of characteristics, such as the material of the core, shell, and surface, more than any individual characteristic, influenced toxicity. Notably, the size of the nanoparticle did not appear significant in determining toxicity across studies. There was an indication that surface charge could affect toxicity, but a distinct relationship between charge and biological response was not identified. Through exploration of the Knowledgebase using the tool, it was determined that it is possible to alter the toxicity of a nanomaterial of a certain core composition by adding different combinations of a shell and/or a functional outer surface, suggesting that proper design choices, as required to achieve a specific function of a material, could mitigate or exacerbate toxicity.

Nano impact

Large datasets containing nanomaterial properties and their fate and effects experimental data are being collected. Visualization tools are needed to analyze these datasets to produce new knowledge from the ever increasing amount of data being generated, but few tools exist. This article describes the development and application of a data visualization tool, N4mics, designed to explore the Nanomaterial-Biological Interactions Knowledgebase. Visualizations generated using N4mics readily reveal that biological responses in the zebrafish assays correlate better with combinations of a shell and/or a functional outer surface than any single property, including size. The tool can be used to quickly visualize the influence of combinations of particle properties on selected toxicity endpoints.

Introduction

The ability to engineer nanoscale materials allows for the development of novel bioactive nanomaterials useful in a myriad of products.[1] The complexity of engineered nanomaterials with regard to their structure, and limitations in instrumentation to fully characterize materials in suspension or in biological assays make it difficult to understand how nanomaterial structure and properties impact biological response, especially in complex media (physiological buffers and cell assay fluids). The similar size scale between biological machinery and nanomaterials, the ability of the exposure medium constituents and biological components (*e.g.* proteins) to coat or otherwise alter nanoparticles *in situ*, and in some cases, the unique properties of nano-scale materials, makes understanding nanomaterial–biological interactions complex and challenging. These challenges are currently hampering the ability to predict biological responses from measured properties of a nanomaterial, and the ability to predict properties of new nanomaterials from the responses of nanomaterials with similar properties, *i.e.* read-across.[2]

Informatics approaches have been suggested as the quickest way to analyze and produce new knowledge using the ever growing amount of data generated during experimental studies of nanomaterial interactions with diverse biological organisms. Unfortunately, a lack of consistent methodology and thorough characterization of materials

[a] *Carnegie Mellon University, Pittsburgh, PA 15213, USA. E-mail: SandraKarcher44@gmail.com*
[b] *Oregon State University, Corvallis, OR, USA*
[c] *Duke University, Durham, NC, USA*
[d] *Carnegie Mellon University, Pittsburgh, PA 15213, USA. E-mail: glowry@cmu.edu*
[e] *Center for Environmental Implications of Nanotechnology (CEINT), USA*

† Electronic supplementary information (ESI) available. See DOI: 10.1039/c6en00273k

frequently precludes direct comparison of results across published studies.[3] What is clear is that numerous material and medium characteristics are important in understanding how nanomaterials will interact with biological systems.[4,5] Large data sets, rich with information on various nanomaterial characteristics and numerous biological responses collected with the same assay and in a defined medium, provide the framework for applying informatics approaches to understanding nanomaterial–biological interactions with the goal of generating novel hypotheses concerning those relationships. Optimal methods of generating new knowledge are often difficult to identify *a priori*; thus, in emerging fields, exploring data in a variety of ways, including using statistical methods and visualization tools, can lead to synergistic outcomes. The development of the NanoInformatics Knowledge Commons (NIKC)[6] is an on-going effort within the Center for the Environmental Implications of NanoTechnology (CEINT) that includes integration of diverse data sets into a central architecture and the development of accompanying applications for data curation, exploration, and visualization.

This article describes the development and application of a data visualization tool designed to explore the results of 151 zebrafish assays stored in the Nanomaterial-Biological Interactions (NBI) Knowledgebase.[7] The Oregon Nanoscience and Microtechnologies Institute (ONAMI), working under the Safer Nanomaterials and Nanomanufacturing Initiative, is using zebrafish assays to examine hazards associated with exposure to nanomaterials and systematically capturing the results of those assays in the NBI Knowledgebase. The small size,[8] optical transparency,[9] availability of genomic data,[10] rapid development,[8] and relatively low husbandry cost of working with zebrafish provide the benefits of a standardized *in vitro* format with the use of whole, living organisms (*in vivo*).[11–13] The zebrafish assay results include observations of mortality and 19 commonly observed sublethal endpoints[12,14–16] for each nanomaterial and exposure scenario, providing a rich database of biological responses that may vary amongst nanomaterials types.

There is general agreement in the literature that waterborne exposure to several types of nanomaterials can be toxic to zebrafish embryos. Asharani *et al.* found a concentration–dependent increase in mortality and a delay in zebrafish hatching when exposed to silver core nanoparticles with starch and bovine serum albumin capping agents[17] and Park *et al.* observed increased mortality and abnormalities in hatching, malformations, and heart rate with exposure to citrate-capped silver nanoparticles.[18] Bai *et al.* also observed increased mortality and retarded hatching with exposure to zinc oxide nanomaterials[19] and Duan *et al.* reported increased mortality and abnormalities in hatching rate and formation as a result of exposure to silica nanomaterials.[14] Results of a 2007 study by Heiden *et al.* demonstrated that dendrimers with amino functional groups (G4), attenuated growth and development of zebrafish embryos at sublethal concentrations; however, dendrimers with carboxylic acid terminal functional groups (G3.5), were not toxic to the zebrafish embryos.[20] Furthermore, they found that arginine–glycine–aspartic acid (RGD)-conjugated G4 dendrimers were less potent in causing embryo toxicity than G4 dendrimers and that RGD-conjugated G3.5 dendrimers did not elicit toxicity at the highest concentrations tested.[20] Harper *et al.* explored the toxic effects of exposure to fullerenes,[21] several metal oxides, and gold nanomaterials.[13,22] Exposure to some of the fullerenes resulted in significant increases in mortality and malformations.[21,22] For the metal oxide nanomaterials tested, about half were benign to zebrafish embryos, but the others significantly increased mortality and morphological malformations.[22] Toxicity associated with exposure to the gold nanomaterials studied was reported to be generally dependent on surface charge; those with no charge (specifically, gold nanoparticles with either MEE (ligand with two ethylene glycol units and a terminal methoxy group or MEEE (three ethylene glycol units and a terminal methoxy group) did not adversely impact the zebrafish but those with either a positive or a negative charge significantly perturbed development, with positively charged particles primarily causing mortality and negatively charged particles inducing malformations.[13] All of these studies indicate that there is a relationship between a nanomaterial's properties and its toxicity potential, but it is difficult to identify the general principles controlling toxicity from any one study.

The goal of the NBI Knowledgebase is to serve as a repository of the zebrafish response data, along with the nanomaterial properties, that can be mined using computational tools to elucidate generalizable relationships between nanomaterial characteristics and associated toxicological responses observed in zebrafish.[11] The experimental method used by ONAMI researchers has been described in the literature.[12,18,23] Particles used in the zebrafish assays are well characterized and made from well-controlled synthesis procedures. By using strict protocols, the study results reported in the NBI Knowledgebase are internally consistent, enabling cross-study comparison of experimental results.

A challenge facing the development of the NBI Knowledgebase is determining how to visualize the large amounts of biological responses with respect to the increasing myriad of particle characteristics. To successfully mine these data, they must be organized and visualized to identify patterns useful in the development of hypotheses and predictive models, and the visualizations must be presented in a way that conveys the complex relationships between material characteristics and biological responses. Developing methods and tools that are effective in leading to new knowledge requires an interdisciplinary collaboration of information technologists, toxicologists, data modelers, and engineers.

The NBI Knowledgebase has been explored by numerous independent groups, with each published analysis showing that nanomaterial characteristics are influencing biological response. Using hierarchical clustering analysis, Harper *et al.* found distinct patterns of toxicity related to both the core composition and the outermost surface chemistry of the nanomaterial, and further concluded that risk assessments

based on the size and core composition of the nanomaterials could be inappropriate.[23] Using RELIEF, a machine learning algorithm, Liu *et al.* concluded that dosage concentration, shell composition, and surface chemistry were the most important indicators of 24 hour mortality in zebrafish.[15] Focusing specifically on zinc oxide nanomaterials, Zhou *et al.*, using principle component analysis and kriging, concluded that intrinsic features of nanoparticles, specifically the presence and/or composition of a capping agent, were useful in the classification and clustering of toxicity data.[24] The visualization tool developed as part of this current work can be used as a companion to other statistical techniques, such as those described above, to explore the NBI Knowledgebase from alternative perspectives, enabling the identification of promising paths of additional computational exploration through the visual testing of alternative hypotheses.

The primary objectives of the current work were to: i) create an interactive informatics tool (N4mics) to explore the NBI Knowledgebase, looking across nanomaterials and across studies; ii) use visualizations to identify correlations between nanomaterial characteristics (including combinations of characteristics) and biological toxicity responses observed in zebrafish; and iii) develop a better understanding of the role computational analysis and visualization tools can play in producing new knowledge.

Methods

For this work, a comprehensive NBI Knowledgebase data set was extracted from the NBI Knowledgebase.[7] One hundred forty eight Excel files were examined. Each file included the zebrafish assay outcomes associated with a specific nanomaterial. Of the 148 nanomaterials, only 36 were dosed at high enough concentrations to generate greater than 99 percent mortality; 54 were dosed at high enough concentrations to generate greater than 50 percent mortality. The design of the NBI Knowledgebase experimental method, and the limitations of making some nanomaterials at high enough concentrations to achieve 100 percent mortality make comparing the toxicity of the different nanomaterials using the lethal concentration (LC) at 50 percent mortality and the no observed adverse effect level (NOAEL), problematic. Without the full dose–response curve, the statistical fitting to the sigmoidal curve covering the range up to and including the concentration that resulted in 100 percent mortality can only be performed using extrapolation. In an attempt to overcome these problems, the NBI Knowledgebase provides two toxicity indicators for each assay at every exposure concentration level, an additive score and a weighted score. The equations and weighting scheme used in the scoring system are described in Liu *et al.*[15] These scores provide insight into the toxicity of each nanomaterial overall, but they cannot be used to identify relationships between nanomaterial characteristics and specific biological responses.

N4mics provides a frontend interface that allows the user to select computational parameters and subsets of data, facilitating the exploration of the NBI Knowledgebase in a variety of ways, including examining the toxicological impact of exposure on individual parts of the zebrafish. To prepare the NBI Knowledgebase for ingestion into the visualization tool, an algorithm was developed to extract data from the Excel files. The extraction algorithm targeted the NBI Knowledgebase particle descriptor, characteristics of the nanomaterials, and the associated biological responses. Nine characteristics were targeted for use in the tool; these were selected based on the number of files in which those characteristics were populated (*i.e.*, contained meaningful information). Additional details regarding the structure of the Excel files are provided on nanoHUB.[25] Descriptions of the targeted characteristics and the number of Excel files in which that characteristic was populated are provided in ESI† (Table S1).

Extracted data from the Excel files were ingested into a MySQL database, conceptualized as represented in Fig. 1. In Fig. 1, the nine nanomaterial characteristics that are the focus of this work are represented in the left most box. The maximum concentration of exposure varied across studies from 30 000 to 55 000 000 parts per billion (ppb). All but seven nanomaterials were studied at concentrations of at least 100 000 ppb. Each study included a control (zero exposure concentration) and up to seven concentrations of exposure covering the range between zero and the maximum concentration, typically a 5-fold dilution. The total number of zebrafish embryos observed at each concentration of exposure remained consistent within a single assay (*e.g.*, if 12 zebrafish were observed in the control, 12 were observed at 16 ppb, 12 were observed at 80 ppb, *etc.*); however, the number of embryos observed varied from assay to assay, with 12 being the minimum and 72 the maximum. Biological responses are observed at two time points, 24 and 120 hours post fertilization (hpf). Abbreviations of biological responses are as follows: Mo – mortality, DP – developmental progression, SM – spontaneous movement, No – notochord malformation, Ax – axis malformation, Br – brain malformation, Ci – circulation, CF – caudal fin malformation, Ey – eye malformation, He – heart malformation, Ja – jaw malformation, Ot

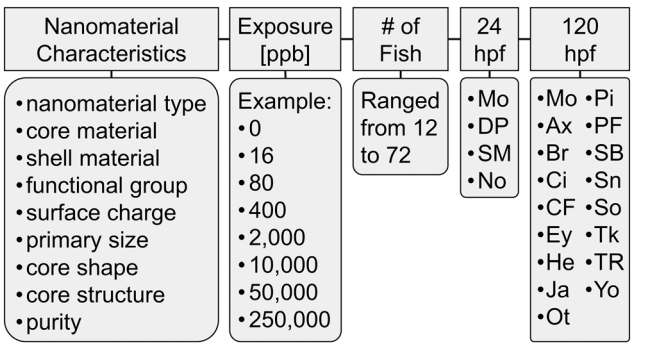

Fig. 1 Conceptual representation of the MySQL database backend used for the visualization tool. Each assay is performed using a specific nanomaterial. Zebrafish are exposed to the nanomaterials over a range of concentrations and the mortality at two time points (24 hpf and 120 hpf) and a total of 19 sublethal responses are observed.

– otic malformation, Pi – pigmentation, PF – pectoral fin malformation, SB – swim bladder, Sn – snout malformation, So – somite malformation, Tk – trunk malformation, TR – touch response, and Yo – yolk sac edema.

After ingestion, data in the MySQL database were prepared for use in the tool. An example of the preparation process for the nanomaterial NBI_6 (Gold-TMAT(1.5 nm)-pure), including the biological responses of mortality and jaw malformation, is provided in Table 1. Table 1 shows the concentrations of exposure used in the assay for this nanomaterial in parts per billion, the number of fish observed to be dead at 24 hpf and 120 hpf, the number of fish that were observed to have a malformation of the jaw at 120 hpf, and the sum of the number of fish that were dead or were observed to have an abnormal jaw at 120 hpf; these are all extracted from the observations reported in the corresponding Excel file. Note that the mortality at 120 hpf is cumulative, meaning that all the fish that died since the beginning of the experiment are included. The number of fish dead at 24 hpf was normalized by the number of fish studied (results shown in column labeled A). The number of fish dead at 120 hpf was also normalized by the number of fish studied (results shown in column labeled B). In this assay, 24 fish were observed at each concentration of exposure. The number of fish observed to have a jaw malformation was normalized by the number of surviving fish (results shown in the column labeled C). Normalizing by the number of survivors provides a means of separating the sublethal responses from mortality observations to allow for direct comparison of the frequency of each sublethal response to all the others as a basis for distinct material-specific comparison of sublethal abnormalities in living fish. The lethal and sublethal responses are summed and normalized by the total number of fish studied (these results are shown in the column labeled D). Eight responses are reported in each column, one for each concentration of exposure including the control. Note also that the last response shown in column C, at the 250 000 ppb concentration of exposure, is shown as 0, but it is actually mathematically undefined because there were no fish still living at 120 hpf. Thus, when normalized by the number of surviving fish, there are only seven valid responses for jaw abnormality. The labels of A, B, C, and D will be used throughout this manuscript to point back to the data preparation and normalization methods shown in Table 1. Each normalization provides different points of comparison and insight into how the properties of the nanomaterials influence biological responses.

The visualization tool guides the user in selecting individual and/or subsets of nanomaterials, responses, and/or characteristics to include in an analysis by providing lists of available options. Using the frontend interface, the user selects relevant computational parameters and indicates how data should be grouped: by nanomaterial (*e.g.*, NBI_6), by response (*e.g.*, jaw), by nanomaterial characteristic (*e.g.*, gold [Au]) or by combinations of nanomaterial characteristics (*e.g.*, {gold [Au] > 2-mercaptoethanesulfonate [MES]}). The characteristics are shown, unless there was a specific reason for changing them, as they were given in the NBI Knowledgebase spreadsheets. When combinations of characteristics are displayed, a greater than sign (>) or double pipes (||) are used to indicate the concatenation of individual characteristics. Herein, combinations of nanomaterial characteristics are shown within curly brackets (*e.g.*, {gold [Au] > 2-mercaptoethanesulfonate [MES]}).

All of the visualizations presented herein aggregate data based on the user selected grouping method and display the distinct groups resulting from that aggregation across the *x*-axis (by nanomaterial number, by response, or by characteristics). Three options are provided for selecting how data are presented along the *y*-axis: (1) by concentration of exposure where responses reach or exceed a target response, (2) by concentration of exposure where the maximum percent response is displayed using a color ramp, and (3) by selected sublethal responses where the maximum percent response observed at concentrations of exposure less than or equal to a user selected threshold concentration is displayed using a color ramp. The three visualization options are described below. Additional details regarding the visualization options are provided on nanoHUB.[25]

Visualization option 1: target response percent graphs

Visualization option 1 performs calculations based on a user specified percentage of fish that exhibit a response and returns a concentration of exposure where that response was met. For the results shown in this paper, a 50 percent response criterion was selected. For an individual nanomaterial, the

Table 1 Example of the data preparation process shown for mortality and jaw abnormalities for the nanomaterial NBI_6 (Gold-TMAT(1.5 nm)-pure)

		A		B			C	D
Exposure [ppb]	# dead fish at 24	% dead to total at 24	# dead fish at 120	% dead to total at 120	# abnormal jaw at 120	# (dead + abnormal jaw) at 120	% abnormal jaw to living at 120	% (dead + abnormal jaw) to total at 120
0	0	0.0	0	0.0	0	0	0.0	0.0
16	0	0.0	0	0.0	0	0	0.0	0.0
80	3	12.5	6	25.0	1	7	5.6	29.2
400	3	12.5	7	29.2	3	10	17.6	41.7
2000	5	20.8	11	45.8	8	19	61.5	79.2
10 000	7	29.2	16	66.7	6	22	75.0	91.7
50 000	11	45.8	20	83.3	3	23	75.0	95.8
250 000	24	100.0	24	100.0	0	24	0.0	100.0

minimum concentration of exposure where 50 percent of the fish are observed to be dead could be considered conceptually similar to the LC_{50} of that nanomaterial, at that specific duration of exposure, with the fundamental difference being that the concentration was determined without being fit to a sigmoidal curve.

Visualization option 1 generates eight graphs, four that present mortality information, two that present sublethal response information, and two that show combined results. The graphs are designed to be read in pairs based on the data preparation method (a pair for preparation method A as shown in Table 1, *etc.*) with each graph visually presenting the results of the underlying analysis in a different way. A simplified, annotated example of the graphs generated by selecting nanomaterial NBI_6 (Gold-TMAT(1.5 nm)-pure), responses of abnormal jaw and mortality is presented in Fig. 2. To develop an understanding of how to interpret the graphs, the results shown in Fig. 2 should be read alongside those shown in Table 1. Notice that each graph is labeled with an A, B, C, or D corresponding to the column of the same name in Table 1. Reading across Table 1, the minimum concentrations resulting in a 50 percent response are 250 000, 10 000, 2000, and 2000 ppb for the data in columns A, B, C, and D, respectively. These values can be obtained from the corresponding exposure graphs (top level) by reading the concentration of the location of the bottom of the dark, solid bar. Notice also in Table 1, the maximum concentrations resulting in, at least, a 50 percent response. For all but column C (% abnormal jaw to living), the maximum occurs at a concentration of exposure of 250 000 ppb. In column C, the maximum occurs at 10 000 and at 50 000 ppb, which displays as up to a maximum concentration of 50 000 ppb on the C.1 graph in Fig. 2.

No abnormal jaw response is shown above 50 000 ppb because there were no fish surviving at the 120 hpf observation at a concentration of exposure of 250 000 ppb. The number that appears over the exposure graphs (top level) indicates the number of levels of exposure concentration (the number of rows in the table) where the percent shown in the correspondingly labeled column in Table 1 is greater than or equal 50. This value, when compared to the total number of exposure concentrations used in the assay, provides insight into the proportion of exposure concentrations in which the target response was met. In column A, only the 250 000 ppb concentration of exposure resulted in a response meeting the 50 percent criterion, thus a "1" is displayed over the bar in graph A.1 (those shown in B.1, C.1, and D.1 were obtained using the same method). The range of exposure for this nanomaterial is shown using the lightly colored gray bar that extends from the *x*-axis up to 250 000 ppb in the exposure graphs (top level).

The columns labeled as A, B, and D in Table 1 show that responses ranged from 0 to 100 percent, and included 8 exposure concentration levels (rows in the table). This range is

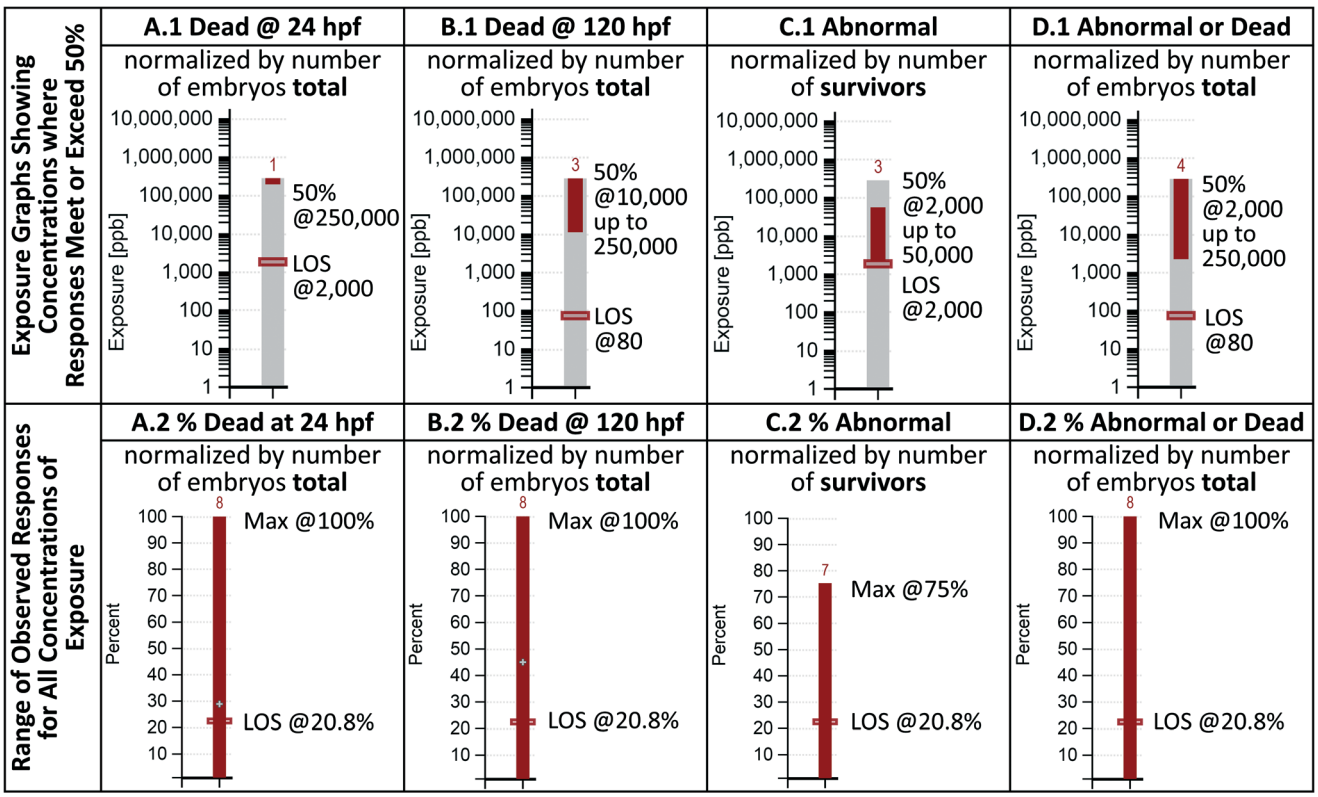

Fig. 2 The annotated exposure and percent graphs (visualization option 1) showing the results for the nanomaterial NBI_6 (Gold-TMAT(1.5 nm)-pure). Biological responses include mortality and jaw malformation. LOS indicates the level of significance as determined using the Fisher's exact test. Exposure graphs (top level) use a 50 percent response criterion.

shown as the solid bar in the corresponding percent graphs (bottom level). The column labeled as C shows a maximum response of 75 percent, and only 7 valid exposure concentration levels (all the fish were dead at the 120 hpf observation of 250 000 ppb). This result is shown on the C.2 graph in Fig. 2. Graphs A.2 and B.2 each display a lightly colored plus sign. The percentage indicated by the plus sign shown on graph A.2 indicates the overall average mortality observed at 24 hpf (the average of the response percentages shown in column A of Table 1) and the percentage shown in graph B.2 indicates the overall average mortality observed at 120 hpf (the average of the response percentages shown in column B of Table 1). Relatively large increases in the average mortality from the 24 to the 120 hpf observation could indicate that the zebrafish are more sensitive to a nanomaterial by oral exposure than through dermal exposure and/or differential susceptibility of the developing zebrafish at different life stages.

To determine if an observed response is large enough to be meaningful, is important to know the minimum exposure concentration where effects begin to manifest in a high enough percentage of the fish to be considered statistically significant. The percent graphs in Fig. 2 (bottom level) show the level of significance (LOS), based on the number of fish observed in the assay, that must show a toxicity response to be considered meaningful. The exposure graphs (Fig. 2 top level) show the corresponding concentration of exposure that first met or exceeded that percentage. These LOS values are based on the Fisher's exact test.[26] The minimum concentration that meets or exceeds the Fisher's exact test response percentage can be considered the lowest observed adverse effect level (LOAEL). For this work, a *p*-value of 0.05 and an on online computational tool by Preacher and Briggs[27] were used to determine the level of significance.

The visualizations generated by the tool are intended to provide insight by reading all the graphs as a unit. When looking at Fig. 2 graphs A.1 and A.2 together, because the 50 percent response was met only at 250 000 ppb (A.1), and 100 percent mortality was reached (A.2), it can be concluded that 100 percent mortality was reached at 250 000 ppb. In contrast, looking at graph B.2, the solid bar indicates that 100 percent mortality was reached, but, because graph B.1 indicates that the 50 percent response was met over a range of exposure concentrations (10 000 to 250 000 ppb) rather than at a single concentration, the 100 percent response could have occurred in any or all of the systems within that concentration range. When looking at the A.1 and B.1 graphs together, a decrease in the minimum concentration of exposure that resulted in 50 percent mortality, from 250 000 ppb at 24 hpf to 10 000 ppb at 120 hpf is observed. A similar reduction, from 2000 to 80 ppb, is observed in the Fisher's exact test level of significance. When looking at the percent graphs, the range of responses all start at zero percent, indicating that no dead fish were observed in the controls at 24 hpf (A.2) or at 120 hpf (B.2), nor were any fish observed to have an abnormal jaw in the controls (C.2), thus the Fisher's percentage level of significance is the same in all the percent graphs (bottom level). Note that a loss of fish in the control experiment would increase the number (percentage) of fish that would have to show an effect to be considered significant. The concentration of exposure required to reach the Fisher's level of significance with regard to sublethal responses is shown on C.1 to be 2000 ppb.

Visualization option 2: concentration gradient heat maps

The second option used for visualizing the NBI Knowledgebase data takes the information from columns A, B, C, and D of Table 1, and applies a color ramp for each response, giving the graph the appearance of a heat map. The heat maps for the nanomaterial NBI_6 (Gold-TMAT(1.5 nm)-pure), including the jaw and mortality responses are shown in Fig. 3. Fig. 3 can be used to gain an understanding of how the biological responses change with exposure concentration. These graphs show the percent response at each exposure concentration. All four of these graphs show an increase in response with concentration. Comparing A.2 (dead at 24 hpf) and B.2 (dead at 120 hpf), the graphs show that both reach 100 percent, with the 120 hpf showing higher responses at the same concentration of exposure as compared to the 24 hpf observations. The C.2 graph indicates that no valid observations were made at the highest concentration of exposure (the total height of the bar is less than in the other graphs). This is because all of the fish were dead at the 250 000 ppb exposure level, and thus, no observation of sublethal abnormalities could be performed. The concentration intervals are aligned so that the bottom of each interval is the actual concentration of exposure where the indicated response was observed. Fig. 3 shows the results for one nanomaterial, thus the color ramp used for each box represents a single value. For example, referring to column A of Table 1, the percent response at 24 hpf is 100 at 250 000 ppb. Fig. 3, graph A.2 shows the darkest shading of the color ramp at a concentration of exposure of 250 000 ppb, indicating a 100 percent response.

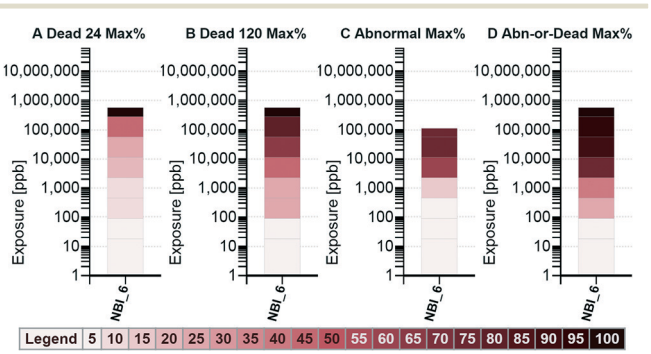

Fig. 3 Exposure concentration heat maps (visualization option 2) showing the results for the nanomaterial NBI_6 (Gold-TMAT(1.5 nm)-pure). Biological responses include mortality and jaw malformation.

Visualization option 3: threshold concentration heat maps

The third option for visualizing the NBI Knowledgebase data takes the information normalized using methods C and D (Table 1), limits the results to those observed at less than or equal to a target concentration threshold and applies a color ramp for the maximum response observed for each sublethal response. Allowing for the selection of a concentration threshold is helpful when looking across studies as a means of equalizing the responses for all assays, even when the maximum exposure concentration used across assays was not uniform. The C.2 heat maps for the nanomaterial NBI_6 (Gold-TMAT(1.5 nm)-pure), including all biological responses, are shown in Fig. 4 using a threshold concentration of 100 000 ppb. Table 1 shows, in column C, that the maximum abnormal jaw response was 75 percent and that this occurred at 10 000 and 50 000 ppb (below the 100 000 ppb threshold); thus, the color ramp used to shade the jaw response indicates a 75 percent maximum response. Exploring data from this perspective provides a means of determining the relative sensitivity of each biological response.

Results

The NBI Knowledgebase was systematically explored to identify how nanomaterial structural features, and combinations of those features correlate with zebrafish responses. Some of the more interesting findings are provided herein. Additional visualizations, including a complete set of visualizations for each of the nine key characteristics individually, more instructions on how to correctly interpret the visualizations, and a fully operational version of the tool are available on nanoHUB.[25]

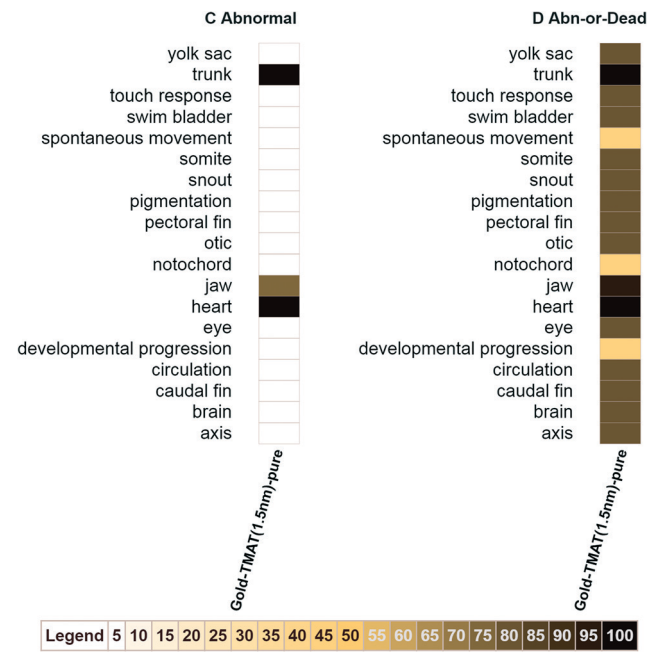

Fig. 4 The biological response heat map (visualization option 3) showing the results for the nanomaterial NBI_6 (Gold-TMAT(1.5 nm)-pure). All sublethal biological responses that meet the threshold target exposure concentration, in this case 100 000 ppb, are included. The color ramp is applied based on the maximum response observed at concentrations less than or equal the threshold.

Visualization of data by general nanomaterial type

To get a sense of the maximum toxicity associated to each general type of nanomaterial, visualizations, including all responses grouped by material type (*e.g.*, dendrimer, metal, polymeric), were generated using a target response of 50 percent. Exposure graphs for option 1 are provided in Fig. 5. From the visualizations, it was observed that the concentration required to reach a 50 percent response was the lowest for the metals group. This indicates that of all the nanomaterials tested, the metal nanomaterial group contained a material that is the most toxic, both with regards to mortality and sublethal impacts.

Dendrimers tended to primarily cause death (50 percent 24 and 120 hpf mortality by 2000 ppb; sublethal response reaching 50 percent only at 10 000 ppb), whereas, the metals and metal oxides caused death and sublethal abnormalities. Carbon, cellulose, and polymeric nanomaterials were relatively less toxic (higher concentrations are required to achieve a 50 percent response), with semiconductor materials falling somewhere in-between.

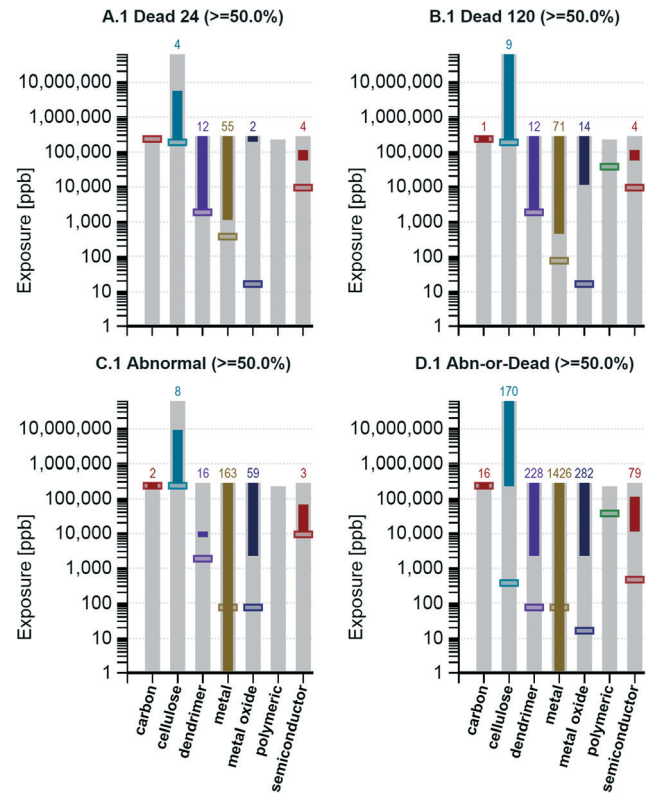

Fig. 5 The exposure graphs (visualization option 1) using a target response criterion of 50 percent. All nanomaterials and all biological responses meeting the target criteria are included. Data are aggregated across the *x*-axis by nanomaterial type.

Visualization of data by nanomaterial core composition

The visualization tool was applied to compare toxicity responses across studies by nanomaterial core composition. The tool output from visualization option 1 is shown in Fig. 6 for the A (dead at 24 hpf), B (dead at 120 hpf), and C (abnormalities) exposure graphs. Note in the *x*-axis label of Fig. 6 that there is a specific type of gold core referred to as "gold [Au]; silver [Ag]". More information on this core combination is provided in the ESI† (Table S1). The minimum concentration required to meet the target response criterion, indicated in Fig. 6 by the bottom of the solid bars, is determined by the most sensitive response endpoint and/or the most toxic nanomaterial in the group. The mortality graphs provided in Fig. 6, A.1 and B.1, show that eight groups contained a nanomaterial that produced a 50 percent response by the 24 hpf observation (those that show a count over a solid bar in A.1) and 13 by the 120 hpf observation (those that show a count over a solid bar in B.1).

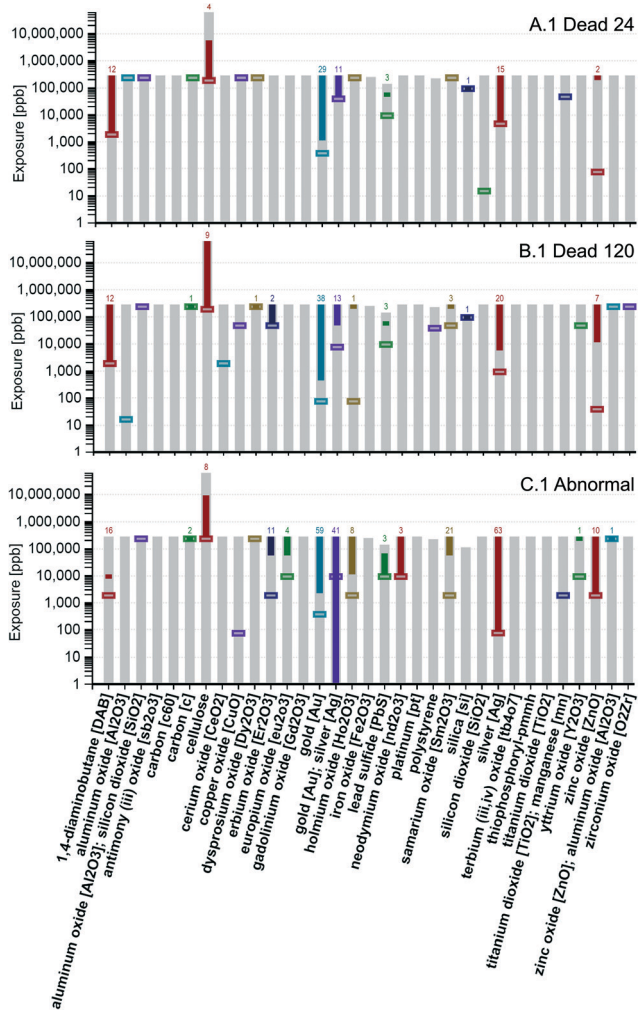

Fig. 6 The concentration of exposure graphs (visualization option 1) for mortality (A and B) and abnormalities (C). All nanomaterials and all biological responses that meet the target criterion of 50 percent are included. Data are aggregated across the x-axis by core material composition.

These 13 are 1,4-diaminobutane [DAB], carbon [c], cellulose, dysprosium oxide [Dy_2O_3], erbium oxide [Er_2O_3], gold [Au], gold [Au]; silver [Ag], holmium oxide [Ho_2O_3], lead sulfide [PbS], samarium oxide [Sm_2O_3], silica [si], silver [Ag], and zinc oxide [ZnO].

Note that the maximum exposure concentration (ranges of exposure shown using light gray bars that start at the *x*-axis) are not the same for all groups. Focusing on the abnormality graph (C.1), it is interesting to note that minimum concentrations needed to achieve a 50 percent response for some of the groups (such as zinc oxide [ZnO] and silver [Ag]), decrease as compared to the minimum concentrations shown in A.1 and B.1 that resulted in 50 percent of the fish dying. In contrast, some groups (such as the gold [Au] group) show an increase in the minimum concentration required to reach a 50 percent response in graph C.1 as compared to A.1 and A.2. These results suggest that the gold [Au] core group contains members that are more likely to kill the zebrafish, whereas, several of the other core groups, such as zinc oxide [ZnO] and silver [Ag] groups, have members that are more likely to harm the zebrafish without killing them. Visualizing the data in this way allows for the comparison of nanomaterial groups by core materials, independent of their coatings.

The percent mortality graphs, A.2 and B.2, are shown in Fig. 7. The graphs in Fig. 7 indicate the average percent mortality across the whole range of exposure using a light colored plus sign. Looking at the samarium oxide [Sm_2O_3] group, it can be seen that the average response increased from 24 hpf to 120 hpf, jumping from 6 to 20 percent. In contrast, the 1,4-diaminobutane group average increased less than 2 percent. Zebrafish move from zygote to hatching in approximately 72 hpf.[28] Up until 120 hpf, diffusion across the skin of the zebrafish is the major route of oxygen supply and of chemical absorption.[13] Around 72 hpf, the zebrafish larva begin to swallow, opening the possibility of exposure *via* ingestion after the 24 hpf observation and before the 120 hpf observation.[13] A relatively large gap in the 24 and 120 hpf averages could be an indicator that the zebrafish are more sensitive to those nanomaterials by oral exposure than they were through dermal exposure and/or of differential susceptibility of the developing zebrafish at these different life stages.

Based on the results shown in Fig. 6 and 7, a correlation between core composition and toxicity cannot be ruled out. It is clear that some core composition groups do not contain a nanomaterial that meets the 50 percent response criterion. Of those that do, the gold, silver, and 1,4-diaminobutane core groups appear to hold the most lethal nanomaterials. From Fig. 6 it can be seen that at least one nanomaterial in these groups killed 50 percent or more of the zebrafish at the lowest concentrations of exposure (5000 ppb or less) and from Fig. 7 it can be seen that at least one nanomaterial in these groups killed 100 percent of the zebrafish.

Fig. 7 shows that other groups also contained at least one nanomaterial that killed 100 percent of the zebrafish. In

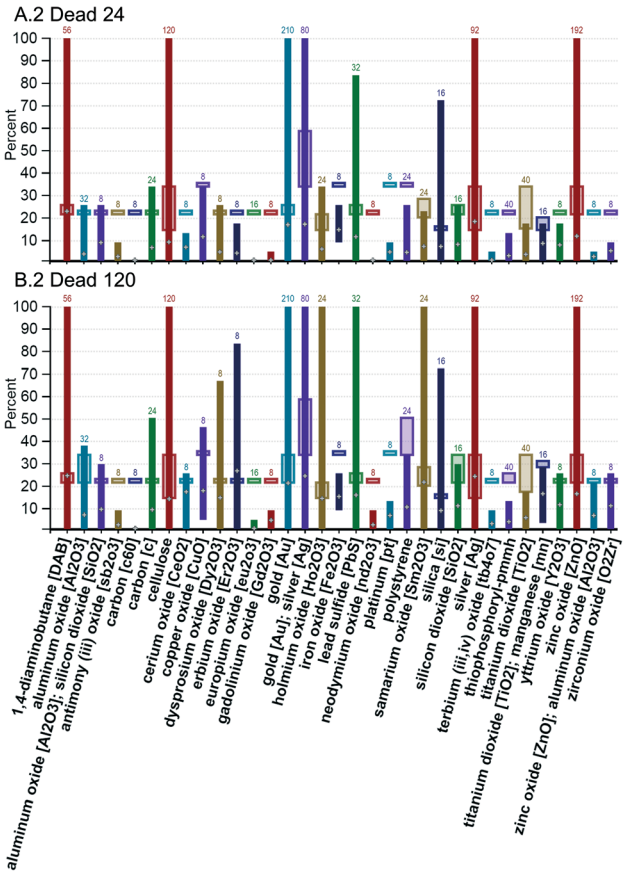

Fig. 7 The percent graphs (visualization option 1) for mortality. All nanomaterials and all biological responses are included. The range of response covers all concentrations of exposure, including the controls. Data are aggregated across the *x*-axis by core material composition.

some cases, Fig. 6 and 7 can be used together to determine the concentration of exposure where the 100 response occurred. For example, Fig. 6, A.1 shows that for the zinc oxide [ZnO] group, a response of 50 percent or greater was achieved at only one concentration of exposure, 250 000 ppb and Fig. 7, A.2, shows that the zinc oxide [ZnO] group reached 100 percent response; thus, it can be inferred that the 100 percent response occurred at the 250 000 ppb exposure. In other cases, the concentration of exposure resulting in the 100 percent response cannot be determined from the graphs shown in Fig. 6 and 7, however, the user could select a 99.9 percent response and rerun the tool and use the revised graphs to determine if and at what concentrations the 99.9 percent response was met or exceeded.

Visualization of data by nanomaterial core, shell, and surface composition

The visualization tool was applied to go one step deeper, from looking only at core composition to comparing toxicity responses across studies by the combination of core, shell, and surface composition. To make the graphs easier to read, only nanomaterials shown to reach 50 percent mortality by the 120 hpf observation (Fig. 6, B.1) and/or that reached a 50 percent response in one or more of the sublethal biological responses (Fig. 6, C.1) were considered. Concentration gradient heat maps generated using all responses and the nanomaterials meeting the 50 percent response criteria are shown in Fig. 8.

Fig. 8 offers some insight into how adding a shell and/or outer surface changes the toxicity of a nanomaterial within a certain core composition group. When data are aggregated, the maximum response in the group is used in applying the color ramp (*i.e.*, the darkest color of all the individual responses is used to determine the shading for the group).

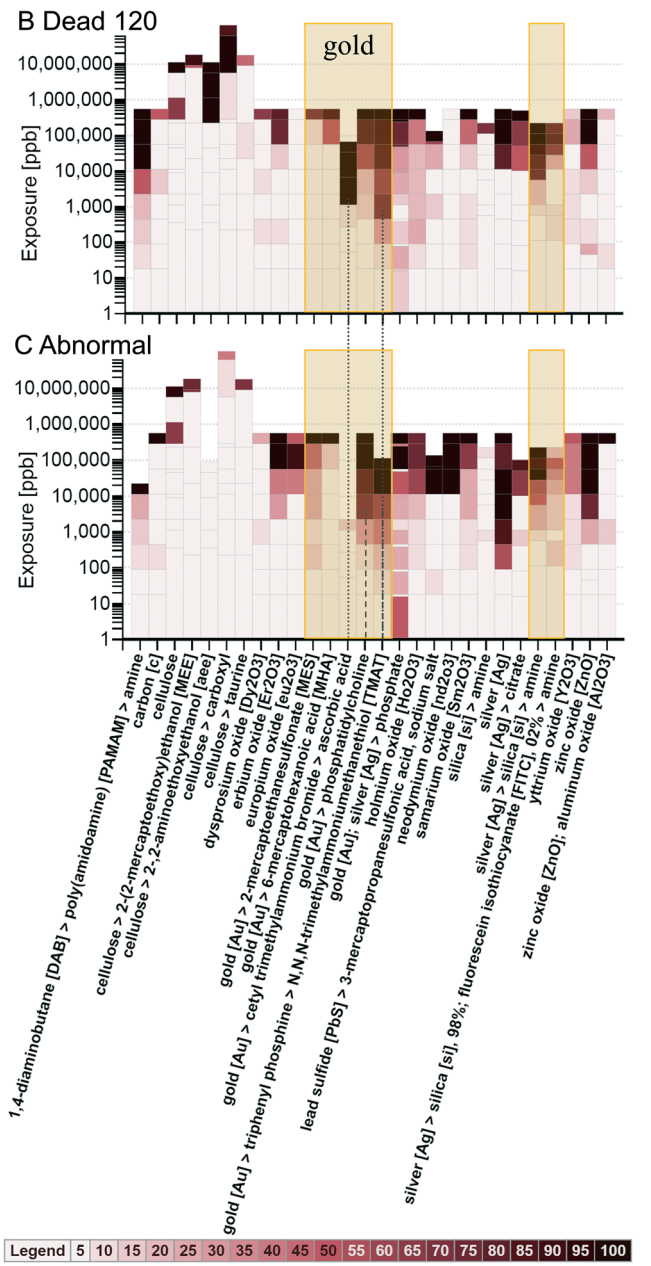

Fig. 8 The concentration gradient heat maps (visualization option 2) for mortality at 120 hpf (B) and abnormalities (C) aggregated by the combination of core, shell, and surface composition for those nanomaterials that reached 50 percent mortality by the 120 hpf observation and/or that reached the 50 percent response criterion in one or more of the sublethal biological responses.

Looking at the gold core nanomaterials (shown in the highlighted boxes), the gold [Au] core with the cetyl trimethylammonium bromide shell and the ascorbic acid surface, and the gold [Au] core with the triphenyl phosphine shell and the *N*,*N*,*N*-trimethylammoniumethanethiol [TMAT] surface (shown with grey dotted lines up to the B.2 graph) show a 50 percent mortality (120 hpf) response at the lowest concentrations of exposure (relative to the other gold core groups). The gold [Au] core with the phosphatidylcholine coating and the gold [Au] core with the triphenyl phosphine shell and the *N*,*N*,*N*-trimethylammoniumethanethiol [TMAT] surface show a 50 percent abnormality response at the lowest concentrations of exposure (shown with grey dashed lines on the C.2 graph), relative to the other gold core groups, except for the gold [Au]; silver [Ag] core with the phosphate surface; however, one of the materials in the gold [Au]; silver [Ag] core group showed abnormalities in the control, and that is influencing the response of the gold [Au]; silver [Ag] core group. Looking at the silver core nanomaterials, the mortality responses appear similar to each other with regard to the concentration at which the 50 percent response was reached, but the uncoated silver [Ag] appears to cause abnormalities at the lowest concentration relative to other silver core groups. It is interesting to note that, with regard to mortality and abnormalities, to achieve responses over 20 percent, the silica [si], 98%; fluorescein isothiocyanate [FITC], 2% shell on a silver core generally requires higher concentrations of exposure to produce the same results as the silica [si] only shell on a silver core, both with an amine surface. Looking at these two in Fig. 8 (shown in the unlabeled highlighted rectangle), it can be seen that, at the same concentrations of exposure, the {silver [Ag] > silica [si] > amine} responses are darker on the color ramp. This suggests that the silica [si], 98%; fluorescein isothiocyanate [FITC], 2% shell leads to reduced toxicity as compared to silica alone. Looking at the cellulose core nanomaterials, from B.1 and C.1 it is evident, based on the color ramp showing little or no response at concentrations of exposure under 100 000 ppb, that the cellulose core nanomaterials are relatively non-toxic to zebrafish regardless of surface chemistry. This is consistent with published literature suggesting that oral and dermal exposure to cellulose nanocrystals is not associated with adverse health effects.[29]

Visualization of data by nanomaterial core, shell, surface composition and surface charge

The visualization tool was applied to examine selected core materials by core, shell, surface chemistry and by surface charge. The B.2 (mortality at 120 hpf) and C.2 (abnormalities) concentration gradient heat maps are provided in the ESI† (Fig. S1 and S2). It is interesting to see how the addition of the shell and/or changes to surface chemistry and charge also change the toxicity of the nanomaterial, but it is difficult to identify a trend. In the gold group (excluding nanomaterials listed in the NBI Knowledgebase as having a gold [Au]; silver [Ag] core), with regard to mortality, the {gold [Au] > triphenyl phosphine > *N*,*N*,*N*-trimethylammoniumethanethiol [TMAT]} (with a positive surface charge), the {gold [Au] > cetyl trimethylammonium bromide > ascorbic acid} (with an unknown surface charge), and the {gold [Au] > phosphatidylcholine} (with a neutral charge) all result in 120 hpf mortality of over 50 percent at concentrations of 10 000 ppb (or less). When looking at the sublethal responses, the {gold [Au] > triphenyl phosphine > *N*,*N*,*N*-trimethylammoniumethanethiol [TMAT]} (with a positive surface charge) and the {gold [Au] > phosphatidylcholine} (with a neutral charge) show responses over 50 percent at concentrations of 2000 ppb. The {gold [Au] > 2-mercaptoethanesulfonate [MES]} (with a negative charge) also reaches the 50 percent response level, but not until the highest concentration level, 250 000 ppb. It is interesting to note that the toxicity of the cetyl trimethylammonium bromide shell is also reported in Li, Huang *et al.* 2009.[30]

When looking at the silver core, the {silver [Ag] > silica [si] > amine} (with a positive charge) results in higher maximum percent response (120 hpf mortality and sublethal) than {silver [Ag] > silica [si] > amine} (with a negative charge) at the same concentrations of exposure above 5000 ppb, but the {silver [Ag] > silica [si] > amine} (with a negative charge) showed some mortality at lower concentrations of exposure, the {silver [Ag] > silica [si] > amine} (with a positive charge) did not. The bare silver [Ag] (with a negative charge) shows equal or greater maximum sublethal responses than all the other silver groups (C.2) at all but one (50 000 ppb) of the exposure concentration levels. When looking at the 1,4-diaminobutane [DAB] core, the {1,4-diaminobutane [DAB] > poly(amidoamine) [PAMAM] > amine} (with a positive charge) shows the highest maximum response for both mortality and sublethal responses. Looking across the cores, these results suggest that the positively charged particles could possibly be correlated with higher mortality, but no such trend can be identified in the sublethal responses. These findings should be further explored using statistical methods to determine if the correlations observed visually are statistically significant.

Visualization of data by a combination of the composition of the surface, shell, and core using a target threshold of 100 000 ppb

To get some insight into how the surface and shell composition alter toxicity, data for all responses and for nanomaterials that reached 50 percent response were aggregated by surface, shell, and core and a relatively high threshold concentration of 100 000 ppb was applied to generate the maximum percent response heat map using visualization option 3.[25] Groups that reached a 50 percent response for one or more of the sublethal responses at concentrations less than or equal 100 000 ppb are summarized in Table 2 (corresponding visualization is provided in Fig. S3 in the ESI†), with the checkmarks indicating the nanomaterial group reached 50 percent for the sublethal response indicated.

These results suggest that nanomaterial exposure can result in a very different pattern of sublethal responses depending on the surface, shell, and core composition. In some groups, combinations of material composition that

Table 2 List of the combinations of surface, shell, and core composition groups with biological responses for which a response of 50 percent was reached at a concentration of exposure of 100 000 ppb or less

Material composition of the combination of surface > shell > core	Ax	Br	CF	Ci	DP	Ey	He	Ja	No	Ot	PF	Pi	Sn	So	SM	SB	TR	Tk	Yo
3-Mercaptopropanesulfonic acid, sodium salt > lead sulfide [PbS]	✓				✓														
Amine > poly(amidoamine) [PAMAM] > 1,4-Diaminobutane [DAB]	✓	✓	✓	✓	✓	✓	✓	✓			✓		✓	✓	✓	✓	✓	✓	✓
Amine > silica [si] > silver [Ag]	✓	✓	✓	✓	✓	✓	✓	✓			✓		✓			✓	✓		✓
Amine > silica [si], 98%; fluorescein isothiocyanate [FITC], 2% > silver [Ag]				✓															
Citrate > silver [Ag]	✓	✓	✓		✓	✓	✓	✓			✓		✓			✓	✓	✓	✓
Erbium oxide [Er_2O_3]						✓	✓	✓					✓						
Europium oxide [Eu_2O_3]	✓		✓				✓												
Holmium oxide [Ho_2O_3]							✓										✓		
N,*N*,*N*-trimethylammoniumethanethiol [TMAT] > triphenyl phosphine > gold [Au]						✓	✓	✓										✓	
Neodymium oxide [Nd_2O_3]																✓			
Phosphate > gold [Au]; silver [Ag]	✓	✓	✓		✓	✓	✓	✓		✓	✓	✓	✓	✓		✓	✓	✓	✓
Phosphatidylcholine > gold [Au]						✓	✓	✓			✓		✓						✓
Samarium oxide [Sm_2O_3]			✓			✓	✓										✓		
Silver [Ag]	✓		✓		✓		✓									✓	✓	✓	✓
Zinc oxide [ZnO]							✓									✓			✓

seem to be similar can result in very different patterns of abnormal sublethal responses. For example, {amine > silica [si], 98%; fluorescein isothiocyanate [FITC], 2% > silver [Ag]} shows a circulation (Ci) response of 50 percent with no other sublethal responses reaching 50 percent, whereas, {citrate > silver [Ag]} shows many sublethal responses over 50 percent, but the circulation response only reached 25 percent. Other groups show similar patterns of responses, such as the {amine > poly(amidoamine) [PAMAM] > 1,4-diaminobutane [DAB]} and the {amine > silica [si] > silver [Ag]} groups. These findings suggest that it might be possible, if enough data were available to support a statistically rigorous analysis, to establish a "fingerprint" of sublethal responses for each combination of material composition, and possibly develop a means of weighting the effect of the core, shell, and outer surface compositions based on the relative pattern of the sublethal responses.

Visualization of data by a combination of the composition of the core, shell, and surface and then by size

The visualization tool was applied to compare toxicity responses by primary particle size. No visual trend was apparent to suggest that particle size is a single predictor of toxicity. To determine if particle size was secondary to core composition as an indicator of toxicity, the tool was used to group data by core composition and particle size. Again, no trend could be identified. When grouped by the combination of core, shell, and surface, and then by size, there is some visual indication that particle size might be important to toxicity, but how size impacted toxicity was difficult to determine. The material combination visualizations are provided in the ESI† (Fig. S4). Fig. S4 shows there was no discernible trend in toxicity with size for {silver [Ag] > silica [si] > amine} nanomaterials (*i.e.* the 67.7 nm particles show greater response at the same concentrations than both the 20 and 69.9 nm materials). Fig. S4 also shows there was no discernible trend in toxicity with size for zinc oxide nanoparticles ranging in size from 4 to 33 nm, however, for materials of the same composition, those of greater size (63 to 76 nm) show increases in mortality at 120 hpf and sublethal response as compared to the smaller sizes (the responses for the three nanomaterials in the 63 to 76 nm range are displayed as darker colors of the color ramp than the responses of the smaller sizes at the same concentrations of exposure). This contradicts the expectation that smaller particles that tend to be more soluble as particle size decreases (*e.g.*, silver[31] and zinc oxide[32]) would be more toxic. Chang *et al.* have previously indicated that the

role of solubility on nanotoxicity, specifically with regard to copper and zinc oxide, is disputable.[33]

Conclusions

The visualizations generated using the N4mics tool show that it is the combination of the composition of the core, shell, and surface, more than any one individually, that influences toxicity. Size does not appear to play a significant role in determining toxicity across nanomaterial core, shell, and surface composition groups, but may play a role within a specific group of materials. There is some indication that surface charge can affect the toxicity of a nanomaterial, but a pattern of how was difficult to identify. What is clear from exploring the NBI Knowledgebase using the visualization tool is that it is possible to alter the toxicity of, or alter the nature of the toxicity (more likely to cause death or cause harm, and what kind of harm is most likely) of a nanomaterial of a certain core composition by adding different combinations of a shell and/or a functional outer surface.

The tool developed as part of the current work provides a frontend interface that guides the user through the process of selecting nanomaterials, responses, and characteristics to include in an analysis and further assists the user in selecting the type of analysis to perform. Multiple analyses can be performed, each using different combinations of nanomaterials, responses, characteristics, response rates, and target concentrations to explore hypotheses related to property-effect relationships. When needed, insights gained from assessing the toxicity of engineered nanomaterials using the tool can be further verified with additional rigorous statistical testing.

The N4mics tool, along with extensive supporting information (including a detailed user's guide), is available on NanoHUB.[25] The NBI source data file, a zip file containing 148 Microsoft Excel files, is also available on NanoHUB.[25] Results of the studies performed on each nanomaterial can also be accessed *via* the NBI Knowledgebase website.[7]

Acknowledgements

The authors acknowledge funding from National Science Foundation (NSF) and the Environmental Protection Agency (EPA) under NSF Cooperative Agreement DBI-1266252 and EF-0830093, the Center for the Environmental Implications of NanoTechnology (CEINT), the National Institute of Environmental Health Sciences (NIEHS) under grant ES017552, and the Air Force Research Laboratory (AFRL) under grant FA8650-05-1-5041 for funding this research. The authors thank Michael Zentner and Steven Snyder for providing technical guidance as part of the CEINTnanoHub listserv and for hosting the N4mics tool on nanoHUB. Finally, the authors acknowledge Elizabeth Casman, Benjamin Colman, Fred Klaessig, Yuan Tian, and Jeanne VanBriesen for providing feedback on earlier versions of the visualization tool. The views, opinions, and content in this article are those of the authors and do not necessarily represent the views, opinions, or policies of their respective employers or organizations to which they maintain membership.

References

1 M. E. Vance, T. Kuiken, E. P. Vejerano, S. P. McGinnis, M. F. Hochella, Jr., D. Rejeski and M. S. Hull, *Beilstein J. Nanotechnol.*, 2015, **6**, 1769–1780.
2 J. H. E. Arts, M. Hadi, M.-A. Irfan, A. M. Keene, R. Kreiling, D. Lyon, M. Maier, K. Michel, T. Petry, U. G. Sauer, D. Warheit, K. Wiench, W. Wohlleben and R. Landsiedel, *Regul. Toxicol. Pharmacol.*, 2015, **71**, S1–S27.
3 J. Rumble and S. Freiman, *Data Sci. J.*, 2012, **11**, ASMD1–ASMD6.
4 V. Maojo, M. Fritts, D. de la Iglesia, R. Cachau, M. Garcia-Remesal, J. Mitchell and C. Kulikowski, *Int. J. Nanomed.*, 2012, **7**, 3867–3890.
5 V. Maojo, M. Fritts, F. Martin-Sanchez, D. De la Iglesia, R. Cachau, M. Garcia-Remesal, J. Crespo, J. Mitchell, A. Anguita, N. Baker, J. Barreiro, S. Benitez, G. De la Calle, J. Facelli, P. Ghazal, A. Geissbuhler, F. Gonzalez-Nilo, N. Graf, P. Grangeat, I. Hermosilla, R. Hussein, J. Kern, S. Koch, Y. Legre, V. Lopez-Alonso, G. Lopez-Campos, L. Milanesi, V. Moustakis, C. Munteanu, P. Otero, A. Pazos, D. Perez-Rey, G. Potamias, F. Sanz and C. Kulikowski, *Comput. Sci. Eng.*, 2012, **94**, 521–539.
6 Center for the Environmental Implications of NanoTechnology, CEINT NanoInformatics Knowledge Commons (NIKC), http://www.ceint.duke.edu/ceint-nanoinformatics-knowledge-commons, (accessed June 26, 2016).
7 Oregon State University, The Nanomaterial-Biological Interactions Knowledgebase, http://nbi.oregonstate.edu/, (accessed December 8, 2015).
8 J. M. Spitsbergen and M. L. Kent, *Toxicol. Pathol.*, 2003, **31**, 62–87.
9 H. Segner, *Comp. Biochem. Physiol., Part C: Toxicol. Pharmacol.*, 2009, **149**, 187–195.
10 A. J. Hill, H. Teraoka, W. Heideman and R. E. Peterson, *Toxicol. Sci.*, 2005, **86**, 6–19.
11 S. L. Harper, J. A. Dahl, B. L. S. Maddux, R. L. Tanguay and J. E. Hutchison, *Int. J. Nanotechnol.*, 2008, **5**, 124–142.
12 L. Truong, S. L. Harper and R. L. Tanguay, *Methods Mol. Biol.*, 2011, **691**, 271–279.
13 S. L. Harper, J. L. Carriere, J. M. Miller, J. E. Hutchison, B. L. S. Maddux and R. L. Tanguay, *ACS Nano*, 2011, **5**, 4688–4697.
14 J. Duan, Y. Yu, H. Shi, L. Tian, C. Guo, P. Huang, X. Zhou, S. Peng and Z. Sun, *PLoS One*, 2013, **8**, 1–9.
15 X. Liu, K. Tang, S. Harper, B. Harper, J. A. Steevens and R. Xu, *Int. J. Nanomed.*, 2013, **8**, 31–43.
16 M. Dellinger, M. J. Carvan, R. H. Klingler, J. E. McGraw and T. Ehlinger, *Challenges*, 2014, **5**, 75–97.
17 P. V. Asharani, Y. LianWu, Z. Gong and S. Valiyaveettil, *Nanotechnology*, 2008, **19**, 1–8.
18 K. Park, G. Tuttle, F. Sinche and S. L. Harper, *Arch. Pharmacal Res.*, 2013, **36**, 125–133.

19 W. Bai, Z. Zhang, W. Tian, X. He, Y. Ma, Y. Zhao and Z. Chai, *J. Nanopart. Res.*, 2010, **12**, 1645–1654.
20 T. C. K. Heiden, E. Dengler, W. J. Kao, W. Heideman and R. E. Peterson, *Toxicol. Appl. Pharmacol.*, 2007, **225**, 70–79.
21 J. B. Pryor, B. J. Harper and S. L. Harper, *Int. J. Nanomed.*, 2014, **9**, 1947–1956.
22 S. Harper, C. Usenko, J. E. Hutchison, B. L. S. Maddux and R. L. Tanguay, *J. Exp. Nanosci.*, 2008, **3**, 195–206.
23 B. Harper, D. Thomas, S. Chikkagoudar, N. Baker, K. Tang, A. Heredia-Langner, R. Lins and S. Harper, *J. Nanopart. Res.*, 2015, **17**, 1–12.
24 Z. Zhou, J. Son, B. Harper, Z. Zhou and S. Harper, *Beilstein J. Nanotechnol.*, 2015, **6**, 1568–1579.
25 S. Karcher, *Informatics Tool to Explore the Nanomaterial-Biological Interactions Knowledgebase*, https://nanohub.org/resources/23991, (accessed May, 2016).
26 J. H. McDonald, *Handbook of Biological Statistics*, Sparky House Publishing, Baltimore, MD, USA, 2009.
27 K. J. Preacher and N. E. Briggs, *Calculation for Fisher's Exact Test: An interactive calculation tool for Fisher's exact probability test for 2 × 2 tables*, http://quantpsy.org, (accessed May, 2016).
28 C. B. Kimmel, W. W. Ballard, S. R. Kimmel, B. Ullmann and T. F. Schilling, *Dev. Dyn.*, 1995, **203**, 253–310.
29 B. J. Harper, A. Clendaniel, F. Sinche, D. Way, M. Hughes, J. Schardt, J. Simonsen, A. B. Stefaniak and S. L. Harper, *Cellulose*, 2016, **23**, 1763–1775.
30 Z. Li, P. Huang, X. Zhang, J. Lin, S. Yang, B. Liu, F. Gao, P. Xi, Q. Ren and D. Cui, *Mol. Pharmaceutics*, 2009, **7**, 94–104.
31 R. Ma, C. Levard, S. M. Marinakos, Y. Cheng, J. Liu, F. M. Michel, G. E. Brown, Jr. and G. V. Lowry, *Environ. Sci. Technol.*, 2012, **46**, 752–759.
32 I. A. Mudunkotuwa, T. Rupasinghe, C.-M. Wu and V. H. Grassian, *Langmuir*, 2012, **28**, 396–403.
33 Y.-N. Chang, M. Zhang, L. Xia, J. Zhang and G. Xing, *Materials*, 2012, **5**, 2850–2871.

